Predictions of the macroscopic model of nuclei: Barriers to fusion and to light fragment emission

N. Carjan and J. M. Alexander
Department of Chemistry, State University of New York at Stony Brook, Stony Brook, New York 11794
and Centre d'Etudes Nucleaires de Bordeaux-Gradignan, 33170 Gradignan, France
(Received 12 May 1988)

Fission and fusion barriers have been calculated for decay or formation of the composite nuclei ^{149}Tb* and ^{194}Hg* via the Yukawa-plus-exponential-finite-range macroscopic model. The predicted properties of these barriers are used for comparisons to measured total kinetic energies for the emission of light fragments ($2 \leq Z_L \leq 9$) and to empirical systematics of s-wave fusion barrier heights. The fusion barriers are consistent with the model. Values of total kinetic energies were calculated with the assumption of no energy loss into excitation beyond the saddle point. For each light fragment, the observed values of total kinetic energies are smaller than those calculated. The deviation increases with Z_L and is correlated with the nuclear shape at the corresponding conditional saddle point. It scales with the neck thickness and the fragment deformation, as does the error involved in our approximation. This suggests (at least for the higher Z_L values) that this macroscopic fission model might apply for light-fragment emission. Dynamical effects must, however, be included.

I. INTRODUCTION

In recent years, macroscopic descriptions of nuclei have been greatly extended and refined. Starting with the basic ideas of the liquid-drop model, Krappe, Nix, and Sierk[1] included the finite (nonzero) range of nuclear forces by means of a Yukawa-plus-exponential attractive potential. The main effect of this refinement on a system undergoing fission or fusion was to reduce its energy, especially in the vicinity of the scission (or touching) point. In the framework of this model, Sierk[2] considered the role of rotational motions, and Davies and Sierk[3] addressed mass asymmetric fissionlike breakup. The model has improved the predictions of fission barriers[4,5,6] that were previously overestimated by the standard rotating liquid-drop (RLD) model,[7] and has accounted for the trend of these barriers for very asymmetric nuclear divisions.[5,6] We will denote this refined macroscopic model as the YEFR model (for Yukawa-plus-exponential finite range).

The YEFR model can also predict barriers for nuclear fusion if one makes an assumption concerning the shapes of the collision partners. For simplicity we will assume that each of the fusing nuclei retains a near-spherical shape until the distance of approach coincides with that for the potential energy maximum. To allow a direct comparison with experiment, fusion barriers are usually defined relative to infinitely separated target and projectile nuclei $B_{\rm fus}^{\infty}$. By contrast, fission barriers are defined relative to the ground state of the fissioning nucleus $B_{\rm fiss}^{\rm CN}$. The energy difference between these two reference states (for zero potential energy) is the Q value for the reaction. Alternatively, one can define fusion barriers relative to the compound nucleus ground state $B_{\rm fus}^{\rm CN}$ or fission barriers relative to the ground state of the separated fragments $B_{\rm fiss}^{\infty}$. These quantities are indicated schematically in Fig. 1. This figure illustrates the potential energy (solid curve) for fission into a particular pair of nuclear fragments ($Z_L, A_L; Z_H, A_H$) and also the potential energy (dashed curve) for the same pair as collision partners in fusion. These barrier heights are different because we have assumed that the fusing nuclei are spherical at the fusion barrier in contrast to fission that is assumed to pass through a saddle-point configuration of shape equilibrium.

The aim of the present study is to compare the predictions of the YEFR model with two observables: (a) the empirical fusion barriers for the formation of the composite nuclei ^{149}Tb* and ^{194}Hg*, and (b) the measured total kinetic energies (TKE's) for light-fragment emission from the same nuclei.

II. BARRIERS TO FISSION

To describe axially symmetric nuclear shapes in this macroscopic model, a Legendre polynomial expansion of $\rho^2(z)$ has been used (with terms up to seventh order in z).[8] Constraining the mass asymmetry degree of freedom to a given value, the saddle point of the resulting six-dimensional potential energy surface was found. The energy of this conditional saddle-point nucleus (relative to that of a spherical nucleus) represents the conditional s-wave barrier to fission. It is calculated with only the macroscopic, shape-dependent terms (i.e., surface and Coulomb). Figure 2 shows calculated fission barriers $B_{\rm fiss}^{\rm CN}$ as well as $B_{\rm fiss}^{\infty}$ versus mass asymmetry parameter η

$$[\eta = |(A_H - A_L)|/(A_H + A_L)]$$

for the composite nuclei ^{194}Hg* and ^{149}Tb*. The YEFR model gives substantially smaller fission barriers than the RLD model, as mentioned in the Introduction. This reduction is much more pronounced for the lighter composite nucleus and for the very asymmetric mass divisions ($\eta \geq 0.6$). It is difficult to extract unambiguous fission barriers from the experimental data available for

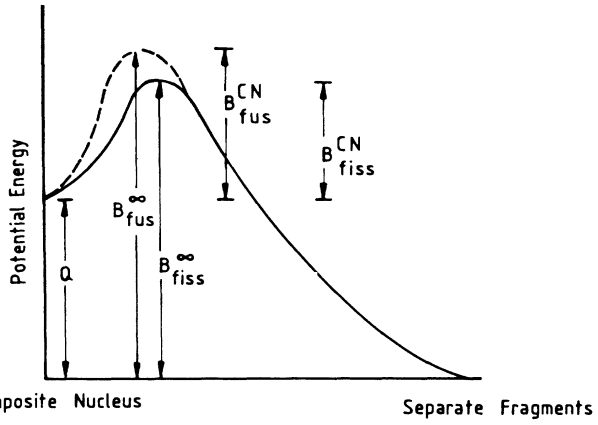

FIG. 1. Schematic diagram of potential energy curves for fission (solid curve) and fusion (dashed curve) for a particular fragment pair. Symbols for various quantities are indicated.

these systems. However, for similar systems, measured fission excitation functions (symmetric fission) are consistent with calculations that employ barriers calculated by the YEFR model.[4] The fact that the observed TKE's in fission[9] are smaller than the calculated values of B^{∞}_{fiss} has long been interpreted as a signal for a viscous descent from the saddle point to a more distended scission-point

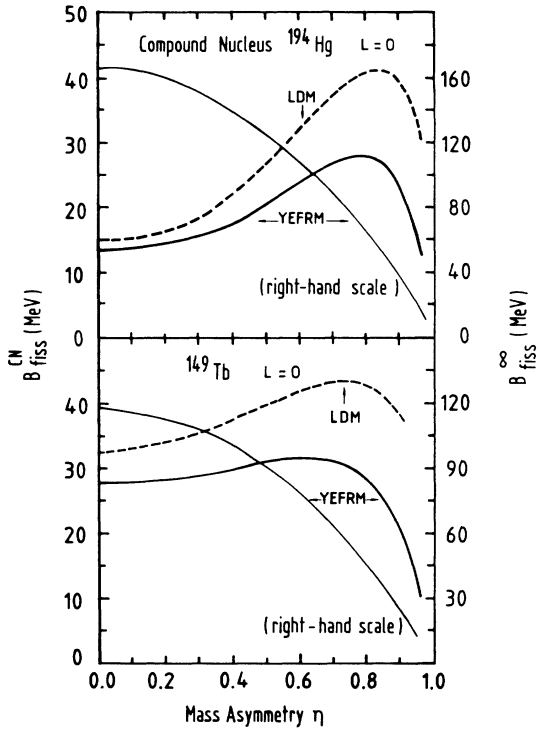

FIG. 2. Fission barriers $B^{\text{CN}}_{\text{fiss}}$ (thick lines, left-hand scale) and B^{∞}_{fiss} (thin lines, right-hand scale) vs mass asymmetry parameter η for the composite nuclei ^{194}Hg* (top) and ^{149}Tb* (bottom). Solid curves were calculated by the YEFR model and dashed curves by the LD model.

configuration. For very asymmetric mass splits, the YEFR model indicates that saddle-point and scission-point configurations become very similar and even approach that for two touching spheres. (See Fig. 3, as discussed herein.) Thus, one might expect that the TKE values (after correction for effects of temperature and spin) would approach B^{∞}_{fiss} and, in the limit, the B^{∞}_{fiss} would approach B^{∞}_{fus}.

III. TOTAL KINETIC ENERGIES FOR EMISSION OF LIGHT FRAGMENTS

Kinetic energy measurements have been reported[10] for emission of light fragments ($2 \leq Z_L \leq 9$); they can also be used to test the conditional saddle-point properties predicted by the model. To calculate the final kinetic energy, one has, in principle, to simulate the dynamical evolution of the fissioning system from the conditional saddle point through scission and on to fully accelerated fragments. However, even without such a detailed dynamical treatment, one can deduce an "upper limit" for the TKE from the conditional barrier height and the saddle-point shape. This calculation is termed an upper limit because energy dissipation and further deformation are neglected. Two methods have been used for this purpose both in conjunction with the YEFR model: (a) the Q-value method and (b) the two-sphere approximation.

(a) The Q-value method.

From Fig. 1 (for a nonrotating system) we see that $B^{\infty}_{\text{fiss}} = B^{\text{CN}}_{\text{fiss}} + Q$; the macroscopic model allows us to calculate $B^{\text{CN}}_{\text{fiss}}$ as well as Q and thus B^{∞}_{fiss}. The $\langle \text{TKE} \rangle$ value, as observed in a particular reaction, will be driven mainly by B^{∞}_{fiss}. For a hot rotating nucleus there will also be contributions from the rotational motion ΔE_{rot}, from the thermal energy, i.e., the initial kinetic energy in the fission decay mode ΔE_{th}, as well as a contribution ΔB from the perturbation of the shape of the saddle-point nucleus due to angular momentum

$$\langle \text{TKE} \rangle = B^{\text{CN}}_{\text{fiss}} + Q + \Delta E_{\text{rot}} + \Delta E_{\text{th}} + \Delta B \ . \tag{1}$$

The correction terms ΔE_{rot} and ΔE_{th} are dependent on assumptions concerning the dynamics of the reaction process. Typically, one views fission as a process of one-dimensional decay along an axis of deformation. This axis can be taken as essentially perpendicular to the spin L of the composite nucleus. Then one can estimate ΔE_{rot} from the condition of rigid rotation

$$\Delta E_{\text{rot}} = [\mu D^2/(\mathcal{I}_1 + \mathcal{I}_2 + \mu D^2)] \times \hbar^2 L(L+1)/2(\mathcal{I}_1 + \mathcal{I}_2 + \mu D^2) \ , \tag{2}$$

where $\mathcal{I}_1$ and $\mathcal{I}_2$ are moments of inertia calculated for spherical fragments, μ is the reduced mass, and D is the fragment separation distance at the saddle point. Similarly, the value of ΔE_{th} is taken from Ref. 11 to be $(\pi/4)T$, which is obtained using Kramer's stationary solution of the one-dimensional Fokker-Planck equation for nondissipative motion.[12] The value of Q is calculated with only the macroscopic terms of the model (as are $B^{\text{CN}}_{\text{fiss}}$ plus ΔB). It is the calculation of $Q_{\text{macroscopic}}$ that distinguishes this approximation for $\langle \text{TKE} \rangle$ from that de-

scribed next.

(b) The two-sphere approximation.

A second estimate has been made by focusing on the calculated shape of the saddle-point configuration. This shape is approximated by two spheres with centers separated by a distance D; the YEFR model is then used to estimate the nuclear plus Coulomb energies of the rotating system. The sum of these potential energies is identified with $B_{\text{fiss}}^{\infty}+\Delta B$ and replaces $B_{\text{fiss}}^{\text{CN}}+Q+\Delta B$ in Eq. (1). As the two-sphere approximation underestimates both the nuclear attraction and the Coulomb repulsion, it is not a rigorous upper limit. However, these errors tend to compensate. As before, this method also neglects dynamical energy losses, and both methods, in this sense, give upper limits to $\langle \text{TKE} \rangle$.

Both methods were applied to the compound nuclei ^{149}Tb* and ^{194}Hg*, and the results are compared to the observed average energies in Figs. 3 and 4. The asymmetry coefficient η of each saddle-point shape was constrained to the value defined by the measured final atomic (or charge) number Z_L. This means that the calculated points correspond to emission of light fragments with initial N/Z ratio of the compound nucleus (since the model assumes a constant N/Z ratio for the whole nucleus from formation to scission). Table I gives these primary average masses A_L for each fragment atomic number Z_L. The data points show Z_L and $\langle \text{TKE} \rangle$ for the final fragments with no correction for particle evaporation. Such a correction would increase both Z_L and $\langle \text{TKE} \rangle$, but leave the trend as shown. For each final fragment, the average angular momentum L of the parent system was obtained from the anisotropy of the measured angular distribution.[10] The temperature of the composite nucleus was calculated for fission as the first step of deexcitation; values are given in Ref. 10. The assumption of fission before neutron emission is not crucial here because the temperature and the calculated barriers change only slowly with neutron number. The very steep excitation functions for these fragments[5] do, nevertheless, give evidence that the very asymmetric fission occurs prior to any appreciable cooling.

Most striking in these figures is the increase with Z_L of the deviations between the calculated upper limits to $\langle \text{TKE} \rangle$ and the experimental values. Examination of the shapes in Figs. 3 and 4 clearly shows that this increase is correlated with the extent of the distention of the nuclear shape at the conditional saddle point (i.e., the neck size and fragment elongation). Such a correlation suggests that the saddle-to-scission dynamics may be responsible for this pattern of deviations. If these light fragments are essentially fission fragments, then an increase of the mass asymmetry should give an approach of the conditional

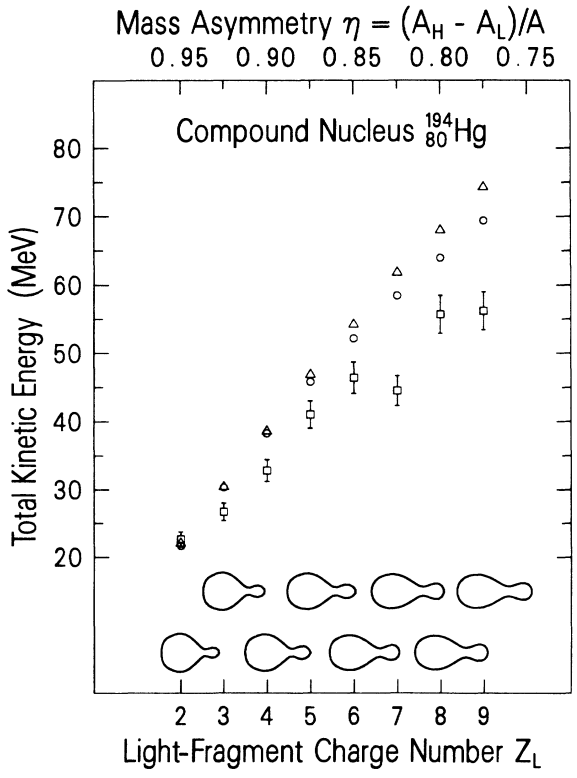

FIG. 3. Comparison between experimental TKE's (Ref. 10) and their estimated upper limits (using YEFR model) for light-fragment emission from ^{194}Hg*. Triangles are used for the Q-value method, circles for the two-sphere approximation, and squares for the experimental data.

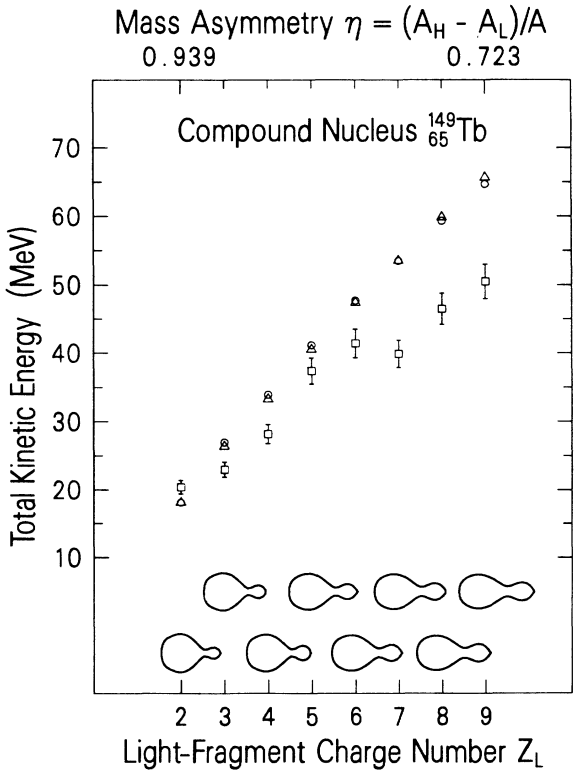

FIG. 4. The same as Fig. 3 except for the composite nucleus ^{149}Tb*.

TABLE I. Average light-fragment mass A_L assumed by the model for each light-fragment charge number Z_L.

Z_L	2	3	4	5	6	7	8	9
A_L (Tb)	4.58	6.88	9.17	11.46	13.75	16.05	18.34	20.63
A_L (Hg)	4.85	7.27	9.70	12.12	14.55	16.97	19.40	21.82

saddle point toward the scission point and the neglected dynamical effects should tend toward zero. This trend does seem to be followed in Figs. 3 and 4.

For the very largest asymmetries (e.g., $Z_L=2$), there is a special sort of dilemma. The α particle is an excellent quantum object (it has small size and strong shell effects). Hence, its emission is not expected to be well described by a purely macroscopic model. Moreover, such an extremely asymmetric saddle-point shape is at (or beyond) the limit of applicability for the current shape parametrization. Therefore, the agreement, in this case, can be taken as fortuitous.

It is interesting, however, that this treatment of He emission does strongly reduce the well-known problem of a surprisingly low emission barrier.[13,14] This result is largely due to our approximation for the magnitude of the temperature-driven part of the TKE. In this treatment one uses a value of $(\pi/4)T$ for $\Delta E_{\rm th}$ for one-dimensional motion along a single fission decay mode. By contrast, treatments of particle evaporation have allowed the emitted particles to have three-dimensional motion in their decay (directions perpendicular as well as parallel to the symmetry axis at scission). These three translational degrees of freedom (equivalent to Hauser-Feshbach coupling[15]), give $\Delta E_{\rm th}\approx 2T$.[10,13,16,17,18] This difference in the dynamical assumptions attributes an additional energy of $\approx(\frac{5}{4})T$ to the thermal-energy driven part of $\langle$TKE$\rangle$.

There are two experimental observations for α-particle emission that are well described by the Hauser-Feshbach coupling commonly used in evaporation models.[14] The first is the Maxwellian shape of the observed energy spectra; the second is the increasing anisotropy with α-particle energy, which is driven (in the model) by the spin dependence of the level density.[14] Hence, we should probably have added $\approx 2T$ instead of $(\pi/4)T$ and the re-

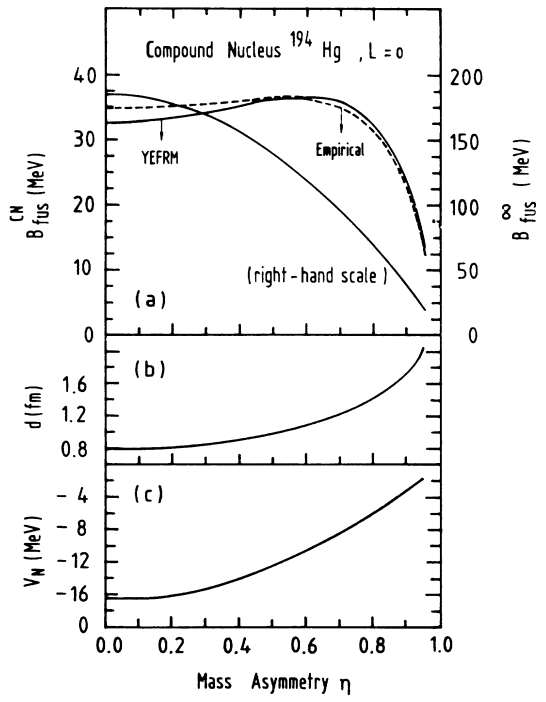

FIG. 5. (a) Fusion barriers $B_{\rm fus}^{\rm CN}$ (left-hand scale) and $B_{\rm fus}^{\infty}$ (right-hand scale) vs η for the composite nucleus ^{194}Hg*. The dashed curve is from the empirical systematics of Ref. 19. (b) The parameter d is the calculated distance between equivalent sharp-surface nuclei at the top of the fusion barrier. (c) Calculated nuclear potential V_N at the top of the fusion barrier.

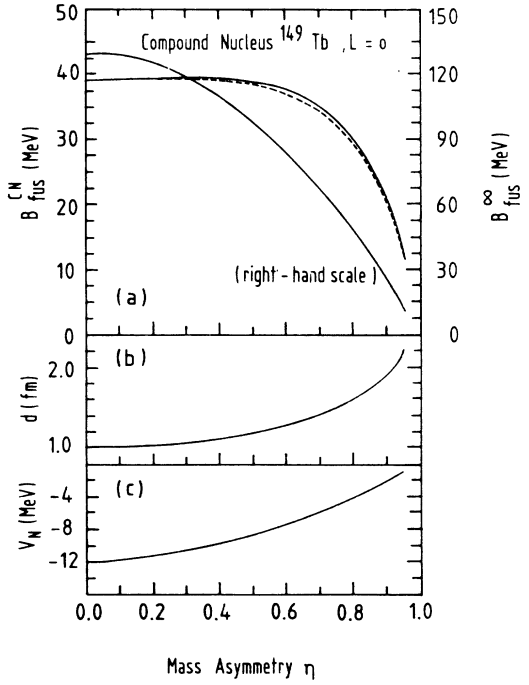

FIG. 6. The same as Fig. 5 except for the composite nucleus ^{149}Tb*.

sulting ⟨TKE⟩ would be, in this case, higher than the measured α-particle energy. As there are no dynamical effects expected for this extreme mass asymmetry to reduce these values, one could infer that, at least for alpha particles, the real emission barrier is lower than the calculated saddle-point barrier.

IV. BARRIERS TO FUSION

Figures 5(a) and 6(a) show calculated fusion barriers $B_{\text{fus}}^{\text{CN}}$ and B_{fus}^{∞} versus mass asymmetry in the entrance channel η. Also shown is a dashed curve taken from empirical systematics of experimental fusion barriers.[19] The close agreement indicates a reasonable consistency with the YEFR potential and the assumption of spherical nuclei at the fusion barrier.

In the YEFR model the fusion barrier can be represented as follows:

$$B_{\text{fus}}^{\infty}=(Z_L Z_H e^2)/[r_0(A_L^{1/3}+A_H^{1/3})+d]+V_N(d)\ , \qquad (3)$$

where $r_0=1.16$ fm, V_N is the nuclear interaction energy, and d is the distance between equivalent sharp surfaces at the barrier maximum. The value of d (for the barrier maximum) was determined by evaluation of B_{fus}^{∞} (Eq. 3) as a function of d. The resulting d values are shown in Figs. 5(b) and 6(b); they vary monotonically from $d\approx 0.8$ fm for $\eta=0$ to $d\approx 2.2$ fm for $\eta=0.95$. This indicates that, in order to fuse, mass symmetric collision partners must approach one another more closely than mass asymmetric ones. However, Fig. 5(a) (for ^{194}Hg*) shows a shallow minimum for $B_{\text{fus}}^{\text{CN}}$ at $\eta=0$. This means that symmetric fusion ($\eta=0$) gives a slightly less excited composite nucleus than does the more asymmetric case of $\eta\approx 0.5$ (for the same entrance channel energy with respect to the barrier height). Fusion with very large mass asymmetry ($\eta\approx 0.95$) can give a composite nucleus of even lower excitation energy because of the very small Coulomb contribution to the fusion barrier. Figures 5(c) and 6(c) show the nuclear interaction energy V_N between fusing nuclei at the maximum in their potential curve. This nuclear potential energy is calculated to be about 9% of the Coulomb energy for both systems and the whole range of η values.

V. DISCUSSION AND CONCLUSIONS

It is very important to understand the mass asymmetry dependence of the properties of nuclei during fission or fusion. For example, it has been suggested that mass asymmetry enables one to distinguish fast fission from equilibrium fission following compound-nucleus formation.[20] Furthermore, statistical-model descriptions of fission and particle decay have been based on rather different assumptions concerning the shapes, excitation energies, and orientations of the transition-state or decision-point nuclei. (See, for example, Refs. 17–19 and references therein.) In particular, some models for nuclear fission have been constructed by assuming that statistical weighting at the saddle point[21] controls the decision process; others have assumed that the statistical control is determined at the scission point.[22]

For the case of symmetric fission of a heavy nucleus, the saddle-point and scission-point configurations are quite different and the choice between them is essential for a model.[18] For very asymmetric fission or for light fissile nuclei, the saddle-point configuration approaches that for scission. Therefore, the problem of this choice is seemingly reduced. In addition, for $\eta\geq 0.85$ the saddle-point shapes approach those of two touching spheres, and thus the fission barriers B_{fiss}^{∞} (Fig. 2) and the fusion barriers B_{fus}^{∞} [Figs. 5(a) and 6(a)] become much closer.

In this work we have calculated fusion barriers with the YEFR model (assuming spherical shapes at the barrier maximum) and showed that they compare well with empirical systematics. Also, we have calculated ⟨TKE⟩ values for the emission of light fragments, assuming no dynamical energy dissipation beyond the conditional saddle point. Our calculations of ⟨TKE⟩ overestimate the experimental results, with the following trend for the deviations: it is negligible for $Z_L=2$ and then increases with Z_L. This trend is indeed what one expects from our macroscopic fission model with no dynamical effects, and it suggests that this model might be applicable for light fragment emission. However, the dynamical effects (in particular, the amount of precision dissipation and fragment deformation at scission) have to be quantitatively estimated before a definitive conclusion on this point can be drawn.

As discussed in Sec. III, it seems that at least for $Z_L=2$, a fission model with one-dimensional decay is not appropriate. Several experimental papers[13,14,23] have shown consistency with three-dimensional decay (Hauser-Feshbach coupling), and in this context the observed values of ⟨TKE⟩ require surprisingly low emission barriers (i.e., 10–30% less than our calculations for B_{fus}^{∞}). This result also seems to imply dynamical distortions (shape, size, vibration, etc.,) of the emitting nuclei away from the idealized configurations of equilibrium. An important current challenge is to understand these exit-channel energies, the associated barriers, and their relationship to macroscopic models.

One should stress that some discrepancies between theoretical and experimental values of the fission barriers are to be expected as there are some important approximations in the current macroscopic approach. Apart from the usual shape-dependent terms (i.e., surface and Coulomb) the macroscopic masses are calculated from several terms that are dependent on nuclear size or nucleonic composition.[24] At scission there is a discontinuity, and both the constant and Wigner terms double their contributions (which for ^{194}Hg* is ≈ 12 MeV). It would be more reasonable to assume that during the fission process all these binding energy terms vary continuously from the value corresponding to the fissioning nucleus to that of the fission fragments. Such a variation would imply an additional "shape dependence." The present (and other existing macroscopic) fission models consider only

one or the other of these two extreme situations, and thus implicitly adopt a discontinuous transition at scission because of these so-called shape-independent contributions. An assumption of continuous variation of the nucleonic binding during fission would modify the deformation dependence of the potential energy, especially close to scission. This would affect both the dynamical descent towards scission as well as the exit-channel barrier heights for light or very asymmetric systems.

ACKNOWLEDGMENTS

We thank A. J. Sierk for the use of his computer programs and for much helpful advice. We also thank R. Nix for his interest in the work and for helpful discussions. This work has been supported in part by the Division of Nuclear Physics, Office of High Energy and Nuclear Physics, U.S. Dept. of Energy and by CNRS of France.

[1]H. J. Krappe, J. R. Nix, and A. J. Sierk, Phys. Rev. C **20**, 992 (1979).

[2]A. J. Sierk, Phys. Rev. C **33**, 2039 (1986).

[3]K. T. R. Davies and A. J. Sierk, Phys. Rev. C **31**, 915 (1985).

[4]J. van der Plicht, H. C. Britt, M. M. Fowler, Z. Fraenkel, A. Gavron, J. B. Wilhelmy, F. Plasil, T. C. Awes, and G. R. Young, Phys. Rev. C **28**, 2022 (1983); F. Plasil, T. C. Awes, B. Cheynis, D. Drain, R. L. Ferguson, F. E. Obenshain, A. J. Sierk, S. G. Steadman, and G. R. Young, Phys. Rev. C **29**, 1145 (1984).

[5]M. A. McMahan, L. G. Moretto, M. L. Padgett, G. J. Wozniak, L. G. Sobotka, and M. G. Mustafa, Phys. Rev. Lett. **54**, 1995 (1985).

[6]A. J. Sierk, Phys. Rev. Lett. **55**, 582 (1985).

[7]S. Cohen, F. Plasil, and W. J. Swiatecki, Ann. Phys. (N.Y.) **82**, 557 (1974).

[8]S. Trentalange, S. E. Koonin, and A. J. Sierk, Phys. Rev. C **22**, 1159 (1980).

[9]V. E. Viola, Jr., Nucl. Data Sec. A **1**, 39 (1966); V. E. Viola, Jr., K. Kwiatkowski, and M. Walker, Phys. Rev. C **31**, 1550 (1985).

[10]L. C. Vaz, D. Logan, J. M. Alexander, E. Duek, D. Guerreau, L. Kowalski, M. F. Rivet, and M. S. Zisman, Z. Phys. A **311**, 89 (1983).

[11]J. R. Nix, A. J. Sierk, H. Hofmann, F. Scheuter, and D. Vautherin, Nucl. Phys. **A424**, 239 (1984).

[12]H. A. Kramers, Physica (The Hague) **40**, 284 (1940).

[13]M. F. Rivet, D. Logan, J. M. Alexander, D. Guerreau, D. Duek, M. S. Zisman, and M. Kaplan, Phys. Rev. C **25**, 2430 (1982).

[14]R. Lacey, N. N. Ajitanand, J. M. Alexander, D. M. de Castro Rizzo, P. DeYoung, M. Kaplan, L. Kowalski, G. La Rana, D. Logan, D. J. Moses, W. E. Parker, G. F. Peaslee, and L. C. Vaz, Phys. Lett. B **191**, 253 (1987); R. Lacey *et al.* Phys. Rev. C **37**, 2561 (1988).

[15]W. Hauser and H. Feshbach, Phys. Rev. **87**, 336 (1952).

[16]L. G. Moretto, Nucl. Phys. **A247**, 211 (1975); L. G. Moretto and R. Schmitt, Phys. Rev. C **21**, 204 (1980).

[17]N. N. Ajitanand, G. LaRana, R. Lacey, D. J. Moses, L. C. Vaz, G. F. Peaslee, D. M. de Castro Rizzo, M. Kaplan, and J. M. Alexander, Phys. Rev. C **34**, 877 (1986); L. C. Vaz, J. M. Alexander, and N. Carjan, Z. Phys. A **324**, 331 (1986).

[18]J. M. Alexander, Ann. Phys. (Paris) **12**, 603 (1987).

[19]L. C. Vaz, J. M. Alexander, and G. R. Satchler, Phys. Rep. **69**, 373 (1981).

[20]C. Gregoire, C. Ngo, and B. Remaud, Phys. Lett. **99B**, 17, (1981), S. Bjornholm and W. Swiatecki, Nucl. Phys. **A391**, 471 (1982).

[21]See, for example, N. Bohr and J. A. Wheeler, Phys. Rev. **56**, 426 (1939).

[22]See, for example, P. Fong, Phys. Rev. **102**, 434 (1956); B. D. Wilkins, E. P. Steinberg, and R. R. Chasman, Phys. Rev. C **14**, 1832 (1976).

[23]U. Gollerthan, H.-G. Clerc, T. Hanelt, W. Moranwek, V. Ninov, W. Schwab, K. A. Schmidt, F.-P. Hessberger, G. Munzenberg, R. S. Simon, J.-P. Dufour, and M. Montoya, Phys. Lett. B **201**, 206 (1988).

[24]See, for example, P. Moller and J. R. Nix, Los Alamos National Laboratory Report LANL LA-UR-86-3983, 1986.